Mechanisms of Hydrogen Exchange of Methane with H-Zeolite Y: An ab Initio Embedded Cluster Study

James M. Vollmer and Thanh N. Truong*

Henry Eyring Center for Theoretical Chemistry, Department of Chemistry, University of Utah, 315 S 1400 E Rm. 2020, Salt Lake City, Utah 84112

Received: March 3, 2000; In Final Form: April 21, 2000

We present ab initio embedded cluster studies on the mechanism of hydrogen exchange of methane with H-Zeolite Y. We found that inclusion of the Madelung field stabilizes the formation of a carbonium-like transition state, and consequently reduces the reaction barrier by 17−23 kJ/mol, relative to the corresponding bare cluster predictions. Using the CCSD(T)/6-31G(d,p) level of theory, including zero-point energy (∼10 kJ/mol) and tunneling (1.6 kJ/mol) corrections, the activation energy is predicted to be 124 ± 5 and 137 ± 5 kJ/mol for hydrogen exchange from two different binding sites. These predictions agree well with the experimental estimate of 122−130 kJ/mol. We also found that it is necessary to include the Madelung potential to find preferrential proton siting at site O1 versus site O4, in agreement with experimental observation.

Introduction

Zeolites are important technological materials due to their many applications. Some important catalytic applications include catalysts for petroleum refining, synfuel production, and petrochemical production.[1−4] The Brønsted acid site has been established as the primary active site for zeolite catalysis; however, little is still known of the mechanistic details for reactions occurring at these sites. For instance, in zeolite catalyzed cracking, isomerization, and alkylation of hydrocarbons, most proposed mechanisms involve proton transfers from the Brønsted site to the hydrocarbon adsorbate to form carbonium (pentacoordinated carbocations) or carbenium ions (tricoordinated carbocations) as reactive intermediates;[5−9] however, there is still little empirical confirmation of the nature of these intermediates.

Hydrogen/deuterium exchange of methane with the Brønsted proton of zeolites has been used as a prototypical reaction of hydrocarbons with zeolites. From a technological point of view, this is an important step in the catalytic conversion of methane to desired products or liquid fuels which is currently one of the greatest challenges in catalysis science. From a fundamental point of view, this reaction is among the simplest elementary processes that can be studied experimentally and theoretically to provide understanding for interactions of hydrocarbons with zeolites at the molecular level. Even for this simple reaction, its mechanism is not yet fully understood, despite numerous studies.

The original experimental and theoretical work for this reaction were reported by Kramer et al. in *Nature* in 1993.[10] By measuring the evolution of the infrared absorption spectrum, the authors were able to extract the isotope exchange rates between CD_4 and the Brønsted proton of H-Zeolite Y and H−ZSM-5 in the temperature range between 620 and 750 K. Their theoretical results from ab initio quantum cluster calculations at the Hartree−Fock (HF) level using a tri-tetrahedral (3T) $H_3Si-OH-Al(OH)_2-O-SiH_3$ cluster did not support the existence of the carbonium-like structure either as the transition state or the intermediate. In fact, the authors reported a transition state structure resembling two free H atoms lying between a CH_3 radical and the zeolite framework. Later theoretical studies done by Evleth et al.,[11] using a 1T (H_2OAlH_2OH) cluster at the HF/6-31G* level of theory, predicted a transition state, whose structure and charge distribution were indicative of $CH_3^-—H_2Z^+$ species (where Z represents the zeolite cluster). Theoretical studies done by Blaskowski et al.,[12] using a 3T ($H_3Si-OH-Al(OH)_2-O-SiH_3$) cluster and various local and nonlocal density functional methods (DFT), with the double ζ plus polarization (DZPV) basis set, and by Truong,[13] using a 3T cluster and a nonlocal hybrid DFT method, both predict transition states similar to Kramer et al. Consequently, to date the nature of the transition state for this reaction is still unclear. All models agree that the transition state geometry resembles a CH_3 fragment, loosely bound to the transferring protons, which are bound to the zeolite framework to some degree. There is, however, still some dispute on the net charge of the CH_3 fragment, as well as the proximity of the exchanging protons to the zeolite framework.

It is not surprising that stable carbonium ion intermediates were not found in these studies, since it is common knowledge that carbocation stability is directly related to the number of alkyl substituents. With no substituents to stabilize it, the CH_5^+ ion is very unstable, and therefore not readily observable. What is surprising is that none of these predictions support a "carbonium ion-like" structure or charge distribution for the transition state, as one would expect based on the typical proton-transfer mechanisms applied to zeolite catalysis. It has been noted that the degree of ionicity of the transition state-lattice interaction is an important parameter, since the more ionic the transition state, the smaller the correlation between activation energy and the differences in proton affinity between the oxygen atom that is deprotonated and the oxygen atom that becomes protonated after the reaction.[4] The implication of this is that the activity differences Kramer et al. simulated for different zeolites, based solely on proton affinity differences between the various active sites, could be perturbed significantly if a more ionic transition state was found.

* Corresponding author. E-mail: Truong@chemistry.utah.edu.

10.1021/jp0008445 CCC: $19.00
Published on Web 06/10/2000

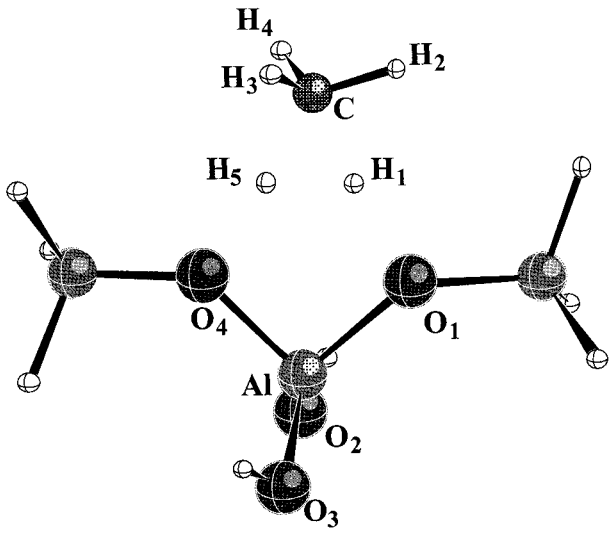

Figure 1. Transition state structure for the proton exchange reaction between methane and Brønsted acid sites O4 and O1 in H-zeolite Y, where the zeolite is represented by a typical 3T cluster. Atom labels are referred to in subsequent tables of structural parameters.

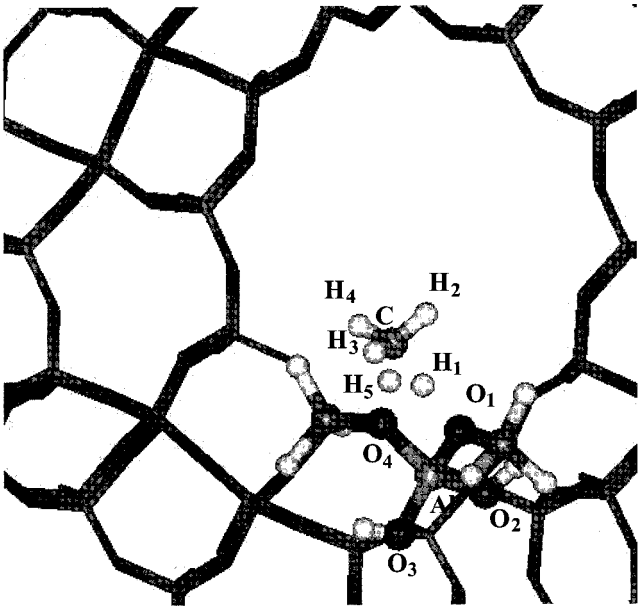

Figure 2. View of our embedded cluster, demonstrating nonequivalent sites O4 and O1 in H-zeolite Y. Atom labels are referred to in subsequent tables of structural parameters.

Previous theoretical studies[14−18] show that inclusion of the zeolite's electrostatic potential is an important factor in stabilizing the $NH_4^+—Z^-$ complex in the zeolite framework, with reaction energies in good agreement with experiment. Thus, the Madelung potential, which is not included in the cluster model, could be a key component to model this hydrogen exchange reaction, since its presence would help stabilize the formation of a more ionic transition state.

Recently we have developed an embedded cluster model, which allows accurate inclusion of the Madelung potential from the extended crystal structure. This model has been successful in studying adsorption of NH_3 in chabazite and H-zeolite Y,[17,18] and of CO in H−ZSM5 and Li−ZSM5.[19] The goal of this study is to use this embedded cluster model to address the above question regarding the effects of the Madelung potential on the mechanism of the hydrogen exchange reaction between methane and H-zeolite Y. In addition, we also examine the proton siting in H-zeolite Y in comparison to neutron and X-ray diffraction studies,[20−22] as well as theoretical studies.[23−25]

Methodology

The details for our embedding scheme have been presented in depth elsewhere, [26] so we will only give a quick overview here. Briefly, we use a 3T quantum cluster ($H_3SiOAl(OH)_2OSiH_3$), cut from the zeolite at the site of interest, where dangling bonds are saturated with H's (see Figure 1). Using a previous study's example we have fixed the length of these dangling bonds at 1.48 Å for Si−H bonds and 1.00 Å for O−H bonds.[14] Local coulomb interactions of the zeolite are included via a set of explicit point charges at lattice sites, where the charge values are derived from a periodic population analysis (Si = 1.97 au and O = −0.985 au).[27] The remainder of the Madelung potential is then represented by a small number of surface charges created within the SCREEP (surface charge representation of the electrostatic embedding potential) methodology.[26] In all, 1285 point charges are used to represent the Madelung potential. All calculations were performed with the nonlocal hybrid BH&HLYP density functional method[28,29] with the 6-31G(d,p) basis set. This level of theory was chosen because it was previously shown to yield excellent agreement with the expensive CISD/6-31G(d,p) method for this same reaction (within 3 kJ/mol).[13] Zero-point energy estimates were achieved by calculating frequencies at all stationary points, using the embedded cluster and BH&HLYP/6-31G(d,p) method. To minimize contributions of the artificial cap H's, we assigned an arbitrarily high mass (1000 a.m.u) to them in these frequency calculations. Basis set superposition error was accounted for by the counter-poise correction (CPC),[30] which was applied at the BH&HLYP/6-31G(d,p) level of theory, by repeating single point calculations at the stationary states, including ghost basis functions, in the calculation of energies for the individual components of the adsorbate complex. Tunneling corrections were previously estimated with the semiclassical small curvature method, for this system.[13] To achieve final estimates for barrier heights, within our embedded cluster model, we performed CCSD(T)/6-31G(d,p) single-point calculations at the BH&HLYP/6-31G(d,p) stationary points.

To represent the steric effects of the zeolite framework, the terminal SiH_3 groups are constrained in the geometry optimizations and transition state searches while the remaining atoms in the quantum cluster are completely relaxed. Note that due to constraints on the SiH_3 groups, the cluster is not symmetric, thus the two oxygen atoms in our 3T cluster (atoms O_1 and O_4) are not equivalent, even in our cluster calculations.

Results

Proton Siting. Zeolite Y is of the Faujasite structure, which has only one unique tetrahedral site (Si or Al) and four corresponding nonequivalent oxygens. In this study we will only look at proton exchange between the O1 and O4 sites in zeolite Y, since these sites point into the zeolite supercage, and are therefore readily accessible for methane adsorption/reaction (see Figure 2). Labels H_1 and H_5 represent the corresponding acidic protons for these two sites. Table 1 shows the differences in geometries between these two sites. Similar to our previous study,[17] the presence of the Madelung field seems to have little effect on the structure of the zeolite framework, as can be seen by the similarities in the geometries for the embedded and bare cluster cases. The largest difference is in the $O_1—O_4$ distance, and corresponding $O_1—Al—O_4$ angle, when the acidic proton

TABLE 1: Geometries of the O4 and O1 Brønsted Sites in H-Zeolite Y (Distances and Angles Reported in angstroms and Degrees, Respectively)

	bare cluster O4 Site	embedded cluster O4 Site	bare cluster O1 Site	embedded cluster O1 Site
$r(H_1O_4)$	0.96	0.96		
$r(H_5O_1)$			0.96	0.97
$r(O_4A_l)$	1.95	1.94	1.72	1.73
$r(O_1A_l)$	1.73	1.74	1.93	1.98
$r(O_4O_1)$	2.62	2.58	2.70	2.58
$\angle O_1AlO_4)$	90.4	89.06	95.2	87.6

TABLE 2: Geometries for Adsorption of Methane at H-Zeolite Y Brønsted Sites (Distances and Angles Reported in angstroms and Degrees, Respectively)

	bare cluster O1 adsorption	embedded cluster O1 adsorption	bare cluster O4 adsorption	embedded cluster O4 adsorption
$r(H_1O_1)$	0.96	0.97	2.63	2.70
$r(H_5O_4)$	2.64	2.70	0.96	0.97
$r(H_1C)$	2.42	2.52	1.09	1.09
$r(H_5C)$	1.09	1.09	2.38	2.39
$r(H_2C)$	1.09	1.09	1.09	1.09
$r(H_3C)$	1.08	1.08	1.08	1.08
$r(H_4C)$	1.08	1.08	1.08	1.08
$r(O_1A_l)$	1.94	1.93	1.72	1.72
$r(O_4A_l)$	1.74	1.73	1.91	1.95
$r(O_1O_4)$	2.63	2.59	2.73	2.62
$\angle(O_4AlO_1)$	91.0	89.7	97.1	90.6

resides at the O4 site. The O_1—O_4 distance is 0.12 Å shorter in the embedded cluster than in the bare cluster case. This shorter distance corresponds to a shorter path the acidic proton must travel for proton transfer, and may foreshadow a lower barrier for proton transfer from this site in the embedded case.

Despite the similarity in geometries, there is a rather significant difference in energetics between the bare cluster and embedded cluster predictions. Using the embedded cluster model, the acidic proton at the O1 site is predicted to be more stable than at the O4 site by 12.0 kJ/mol. In contrast, bare cluster calculations predict the acidic proton at the O4 site to be favored by 6.4 kJ/mol over that of the O1 site. A few theoretical studies have investigated the question of proton siting in H-zeolite Y.[23−25] All studies are in agreement with our embedded cluster results, predicting the proton to be more stable at site O1 than O4 by: 51 kJ/mol, using CNDO/2 semiempirical method;[23] 18.4 kJ/mol, performing lattice energy minimizations with shell model potentials;[24] and 54.1 kJ/mol, performing lattice energy minimizations with van Santen et al.'s potential parameters.[25]

A recent neutron powder diffraction studies has been able to directly determine the positions and occupations of the proton sites in H-zeolite Y.[22] For the most part, these findings are in good agreement with previous inferences of the proton positions and occupations based on X-ray and neutron diffraction studies.[20,21] All of these studies predicted 0% occupation at site O4, with the exception of one sample which found 11% of the sites occupied. In contrast, all of these studies found the O1 sites to be populated to a much larger degree, with occupations ranging from 39 to 54% of the sites. Thus, the inclusion of the Madelung potential is important for obtaining the correct order of preferential proton sitings. Furthermore, these results indicate that *inclusion of steric constraints alone in cluster calculations is not enough to reproduce the effects of the zeolite framework on energetics.*

Adsorption Complexes. Both methods predict adsorption minima for methane at the O1 as well as the O4 sites. Table 2 presents the geometries for these adsorption complexes. There is little difference between the structures predicted by the bare and embedded cluster methods, with the most noticeable difference being the O_1—O_4 distance, when CH_4 is adsorbed at the O4 site. A shorter distance is found within the embedded cluster formalism, being 0.11 Å shorter than that found with the bare cluster method. Another parameter that varies to a large extent between the two methods is $r(H_1C)$, for adsorption at site O1. In the embedded case, $r(H_1C)$ is 0.10 Å longer than in the bare cluster case, which is reasonable since the Madelung potential partially stabilizes the adsorption complex, so that it is not bound as tightly to the zeolite wall. Note that $r(H_5C)$, during adsorption at site O4, differs by only 0.01 Å for the two methods. Perhaps this asymmetric behavior is due to the more acidic nature of the Brønsted proton at site O4. Above it was noted that within the embedded cluster model the proton affinity of site O4 is weaker than that of site O1 by 12.0 kJ/mol, so conversely the acidity of site O4 is stronger to the same extent. Since this site is more acidic, we would expect it to interact more strongly with the methane, and consequently, the hydrogen bond between the zeolite and methane would be shorter.

The calculated adsorption energies, using the embedded cluster model are: −12.0 and −10.3 kJ/mol, at sites O4 and O1, respectively. Using the bare cluster method, the predicted adsorption energies are: −9.2 and 1.7 kJ/mol, at sites O4 and O1, respectively. Both methods predict very weak interactions between the methane and the zeolite Brønsted site, with the strongest binding occurring at the O4 site. The predicted adsorption energies at site O4 are comparable for both methods, however, at site O1 they differ by 12.0 kJ/mol, with the bare cluster method actually yielding a positive adsorption energy. This positive adsorption energy is due to the constraints imposed on the terminal SiH_3 groups of the cluster. By releasing these constraints and performing full geometry optimizations an adsorption energy of −8.1 kJ/mol was found for adsorption at this site.

TABLE 3: Comparison of the Geometries and Charge Distributions for the Transition State of Hydrogen Exchange of Methane at H-Zeolite Y Brønsted Sites (Distances and Angles Reported in angstroms and Degrees, Respectively, and Charges in au)

	isolated CH_5^+	embedded 3T	3T cluster	1T cluster[a]
$r(H_1O_1)$		1.45	1.32	1.16
$r(H_5O_4)$		1.42	1.32	1.16
$r(H_1C)$	1.19	1.26	1.32	1.50
$r(H_5C)$	1.19	1.26	1.31	1.50
$r(HC)$	1.09	1.09	1.09	1.09
$r(O_1Al)$		1.80	1.83	1.86
$r(O_4Al)$		1.82	1.83	1.86
$\angle(O_4AlO_1)$		92.0	91.6	
$q(H_1/H_5)$	0.33	0.37	0.37	0.26
$q(H)$	0.31	0.21	0.17	0.16
$q(C)$	−0.59	−0.63	−0.66	−0.77
$q_{net}(C)$	1.00	0.67	0.21	(∼−0.03)

[a] Reference 11 using HF/6-31G(d).

Is the Transition State a Carbonium Ion? To answer the question regarding the nature of the transition state we focus this discussion on the geometry and charge distribution of the transition state. Table 3 presents the BH&HLYP transition state geometries, using both the bare and embedded cluster methods, as well as previous theoretical results[11] for this system. The important geometrical parameters are $r(H_1O_1)$, $r(H_5O_4)$, $r(H_1C)$, and $r(H_5C)$ (see Figures 1 and 2 for atom labels). These parameters identify the relative positions of the exchanging protons (H_1 and H_5) in the transition state. In our bare cluster calculations we find a transition state nearly identical to those

TABLE 4: Comparison of Classical ($\Delta V^{\ddagger}$) and Zero-Point Energy Corrected ($\Delta V_a^{G\ddagger}$) Barrier Heights (kJ/mol), for Hydrogen Exchange with CH_4/CD_4 between the O1 and O4 Brønsted Sites of H-Zeolite Y

model	adsorbate	level of theory	$\Delta V^{\ddagger}$ from O4	$\Delta V_a^{G\ddagger}$ from O4	$\Delta V^{\ddagger}$ from O1	$\Delta V_a^{G\ddagger}$ from O1
embedded cluster	CD_4	BH&HLYP/6-31G(d,p)	139.0	129.2	151.0	141.1
3T cluster model	CD_4	BH&HLYP/6-31G(d,p)	168.1	156.9	161.7	150.9
1T cluster model	CH_4	MP2/6-31++G(d)//HF/6-31G(d)[a]	166.8	152.6	166.8	152.6
3T cluster model	CH_4	HF/6-31G(d,p)[b,d]	236.3		236.3	
1T cluster model	CH_4	CISD/6-31G(d,p)[b,d]	174.2		174.2	
3T cluster model	CH_4	LDA/DZPV[c]	51.6	41.2	51.6	41.2
3T cluster model	CH_4	BP/DZPV[c]	131.6	121.2	131.6	121.2
1T cluster model	CH_4	BP-SCF/DZPV[c]	137.4	125.1	137.4	125.1

[a] Taken from ref 11. [b] Taken from ref 31. [c] Taken from ref 12 [d] Used adsorbed CH_4 as reference minima instead of free acid site, but adsorption energies are low enough (~ -3 kJ/mol) that comparison is still reasonable

reported by previous cluster studies[10,12,31] where the exchanging protons are shared equally between the zeolite and the methane molecule, with $r(H_1O_1) = r(H_5O_4) = r(H_1C) = r(H_5C) = 1.32$ Å. The Madelung potential noticeably shifts the relative locations of the exchanging protons at the transition state away from the zeolite framework. In the embedded case, $r(H_1O_1)$ and $r(H_5O_4)$ are 0.13 and 0.10 Å longer, respectively, than our corresponding cluster predictions. The embedded predictions for these parameters are also 0.26−0.29 Å longer than those predicted by Evleth et al.,[11] using a 1T cluster model at the HF/6-31G(d) level. In addition, $r(H_1C)$ and $r(H_5C)$ are 0.06 and 0.05 Å shorter in the embedded cluster case than those in the analogous cluster results, and are also shorter than all other cluster predictions. Also, when compared to the structure of free CH_5^+ (in Table 3), the embedded cluster's transition state structure is closer for the CH_5 moiety than any of the bare cluster predictions.

The Mulliken population (in Table 3) for the embedded cluster's transition state also agrees more closely to the free CH_5^+ ion than the cluster predictions. To examine the net charge on the carbon atom, $q_{net}(C)$, the hydrogen atoms' charges were summed into their nearest heavy atom neighbors. This analysis was not presented in Evleth et al.'s original report, so we approximated their values by evenly dividing the charge of the exchanging protons (H_1 and H_5) between the carbon and oxygen atoms. This will slightly overestimate the carbonium nature of their transition state since the exchanging protons in the cluster models are actually closer to the zeolite oxygens than the carbon atom; however, it does not alter the conclusion. In the BH&HLYP cluster case an effective charge of only 0.21 au resides on the carbon atom, verses the 1.00 au expected for a carbonium ion species. Although slightly positive, these charges in conjunction with the predicted structures, seem more consistent with a covalently bound hydrocarbon fragment or radical than a carbonium ion. The 1T cluster model at the MP2/6-31++G(d,p)//HF/6-31G(d) level yields significantly different results. It predicts a net negative charge on the carbon atom. In our embedded cluster calculations, the transition state is significantly more ionic than the present and previous cluster predictions, with more than three times as much positive charge (0.67 au) effectively lying on the carbon atom. The charge is not 1.00 au as would be the case for an isolated CH_5^+ molecule, because the adsorbate species is bound to the zeolite framework, yet it is positive enough to display definite ionic character. So the Madelung potential promotes the carbonium-character in the transition state of this hydrogen exchange reaction.

Effect of the Madelung Potential on Barrier Heights. Calculated barrier heights, along with those from previous studies, are listed in Table 4. To be consistent with previous studies, the reported barriers are relative to the isolated Brønsted sites and isolated methane instead of the adsorption complex.[10−13] On the basis of the discussion above, we would expect the Madelung potential to lower the reaction barrier, due to the ionic nature of our transition state. In fact, the Madelung potential reduces the barrier heights by 10.7 kJ/mol from the O1 site and by 29.1 kJ/mol from the O4 site, relative to the bare cluster calculations. In more quantitative terms, the CCSD(T)//BH&HLYP classical barriers are 132.5 and 144.4 kJ/mol for hydrogen exchange from the O4 and O1 sites, respectively. The BH&HLYP method yields good barrier heights, lying only 6.5 kJ/mol too high, relative to the CCSD(T) results. Including zero-point energy corrections, the barrier heights are further reduced by approximately 10 to 12 kJ/mol; however, applying the counterpoise correction increases the barrier heights by 7 to 8 kJ/mol. From our previous study,[13] using the accurate multi-dimensional semiclassical small curvature tunneling method,[32] we found that tunneling can further reduce the barrier by an additional 1.6 kJ/mol in the experimental temperature range of 620−750 K. We also must consider deviations arising from our treatment of steric constraints at the boundary of the quantum cluster. By fixing the terminal SiH_3 groups of the cluster we are over-estimating this constraint. Above we demonstrated that the binding of CH_4 was increased by 9.8 kJ/mol when these constraints were removed in the bare cluster calculations, so we can estimate deviations in the barrier heights due to these constraints to be less than 9.8 kJ/mol. Including all of these corrections, we arrive at barrier heights of 124 ± 5 and 137 ± 5 kJ/mol for hydrogen exchange from sites O4 and O1, respectively. Note that our proton siting results found the Brønsted site to be more stable at O1. Considering the relative energetics of the two proton sites, we can approximate the effective activation energy by considering the Boltzmann distribution between these sites at 650 K (90.2% at site O1 and 9.8% at site O4), and weight the barriers accordingly. In this manner we arrive at a final estimate of 136 ± 5 kJ/mol for the effective barrier height, in agreement with the experimental estimates of 122−130 kJ/mol.[10,4]

Comparing the present results with previous theoretical studies (see Table 4),[10−12,31] the BP/DZPV and BP−SCF/DZPV barrier heights are also within the experimental range of 122−130 kJ/mol. This might lead to the conclusion that the Madelung potential is not essential for this reaction; however, in a previous systematic study[33] on the performance of different DFT methods for studying reactions of this nature, it was found that the Becke[34]−Perdew[35] (BP) method tends to underestimate barrier heights by approximately 30 kJ/mol. Such a finding is consistent with the results for the present hydrogen exchange reaction, for the BP/DZPV and BP−SCF/DZPV methods predict barriers ~30 kJ/mol lower than those from the present BH&HLYP/6-31G(d,p) and CCSD(T)/6-31G(d,p) calculations, and the previous CISD/6-31G(d,p) result.[31] The other previous studies all

present barriers in good agreement with our bare cluster predictions.

Conclusions

In this study, we have employed an accurate ab initio embedded cluster model to study the mechanism of the hydrogen exchange reaction between CH_4 and Zeolite H−Y. We found the transition state has carbonium-like characteristics from both geometrical and electron density considerations. This increased carbonium character is due to inclusion of the Madelung potential, which was neglected in the previous cluster calculations. The Madelung potential is also responsible for predicting site O1 to be the preferred site for the Brønsted proton, over O4, in agreement with theoretical and experimental findings. The embedding potential reduces the barrier for this reaction by approximately 17−23 kJ/mol, relative to the corresponding bare cluster predictions. Including zero-point energy (∼10 kJ/mol), the counterpoise correction (7−8 kJ/mol), and tunneling corrections (1.6 kJ/mol), we predict the activation energies to be 124 ± 5 (from site O4) and 137 ± 5 kJ/mol (from site O1), in good agreement with the experimental range of 122−130 kJ/mol. This study demonstrates the advantages of the ab initio embedded cluster method in modeling the nature of zeolite active sites, adsorptions, and catalytic reactions occurring at these sites.

Acknowledgment. This work is supported in part by the University of Utah and the National Science Foundation. An allocation of computer time from the Center of High Performance Computing at the University of Utah is gratefully acknowledged.

References and Notes

(1) van Bekkum, H., Flanigen, E. M., Jansen, J. C., Eds. *Introduction to Zeolite Science and Practice*; Elsevier Science Publishers: Amsterdam, 1991; Vol. 58.
(2) Sauer, J. *Chem. Rev.* **1989**, *89*, 199−255.
(3) Sauer, J.; Ugliengo, P.; Garrone, E.; Saunders, V. R. *Chem. Rev.* **1994**, *94*, 2095−2160.
(4) van Santen, R. A.; Kramer, G. J. *Chem. Rev.* **1995**, *95*, 637−660.
(5) Haag, W. O.; Dessau, R. M. In *Proceedings of the 6th International Congress on Catalysis*; Berlin, 1984; VZ, p 305.
(6) Haag, W. O.; Lago, R. M.; Weisz, P. B. *Nature* **1984**, *309*, 589.
(7) Jacobs, P. A.; Martens, J. A. In *Introduction to Zeolite Science and Practice*; van Bekkum, H., Flanigen, E. M., Jansen, J. C., Eds.; Elsevier: Amsterdam, 1991; pp 445−496.
(8) Abbot, J.; Wojciechowski, B. W. *J. Catal.* **1989**, *115*, 1−15.
(9) Stefanidis, C.; Gates, B. C.; Haag, W. O. *J. Mol. Catal.* **1991**, *67*, 363−367.
(10) Kramer, G. J.; van Santen, R. A.; Emeis, C. A.; Nowak, A. K. *Nature* **1993**, *363*, 529−531.
(11) Evleth, E. M.; Kassab, E.; Sierra, L. R. *J. Phys. Chem.* **1994**, *98*, 1421−1426.
(12) Blaszkowski, S. R.; Jansen, A. P. J.; Nascimento, M. A. C.; van Santen, R. A. *J. Phys. Chem.* **1994**, *98*, 12938−12944.
(13) Truong, T. N. *J. Phys. Chem. B* **1997**, *101*, 2750−2752.
(14) Greatbanks, S. P.; Sherwood, P.; Hillier, I. H.; Hall, R. J.; Burton, N. A.; Gould, I. R. *Chem. Phys. Lett.* **1995**, *234*, 367−372.
(15) Brändle, M.; Sauer, J. *J. Mol. Catal. A: Chem.* **1997**, *119*, 19−33.
(16) Brändle, M.; Sauer, J. *J. Chem. Phys.* **1998**, *109*, 10379−10389.
(17) Vollmer, J. M.; Stefanovich, E. V.; Truong, T. N. *J. Phys. Chem. B* **1999**, *103*, 9415−9422.
(18) Vollmer, J. M.; Truong, T. N. *J. Comp. Chem.* Submitted for publication.
(19) Limtrakul, J.; Khongpracha, P.; Jungsuttiwong, S.; Truong, T. N. *J. Mol. Catal. A* **2000**, *153*, 155.
(20) Olson, D. H.; Dempsey, E. *J. Catal.* **1969**, *13*, 221.
(21) Jirak, Z.; Vratislav, S.; Bosacek, V. *J. Phys. Chem. Solids* **1980**, *41*, 1089.
(22) Czjzek, M.; Jobic, H.; Fitch, A. N.; Vogt, T. *J. Phys. Chem.* **1992**, *96*, 1535−1540.
(23) Dubsky, J.; Beran, S.; Bosacek, V. *J. Mol. Catal.* **1979**, *6*, 321−326.
(24) Schröder, K. P.; Sauer, J.; Leslie, M.; Catlow, C. R. A.; Thomas, J. M. *Chem. Phys. Lett.* **1992**, *188*, 320.
(25) Kramer, G. J.; van Santen, R. A. *J. Am. Chem. Soc.* **1993**, *115*, 2887−2897.
(26) Stefanovich, E. V.; Truong, T. N. *J. Phys. Chem. B* **1998**, *102*, 3018−033.
(27) Nicholas, J. B.; Hess, A. C. *J. Am. Chem. Soc.* **1994**, *116*, 5428−5436.
(28) Becke, A. D. *J. Chem. Phys.* **1993**, *98*, 1372.
(29) Lee, C.; Yang, W.; Parr, R. G. *Phys. Rev. B* **1988**, *37*, 785.
(30) Boys, S. F.; Bernardi, F. *Mol. Phys.* **1970**, *19*, 553.
(31) Kramer, G. J.; van Santen, R. A. *J. Am. Chem. Soc.* **1995**, *117*, 1766−1776.
(32) Lu, D. H.; Truong, T. N.; Melissas, V. S.; Lynch, G. C.; Liu, Y. P.; Garrett, B. C.; Steckler, R.; Isaacson, A. D.; Rai, S. N.; Hancock, G. C.; Lauderdale, J. G.; Joseph, T.; Truhlar, D. G. *Comput. Phys. Commun.* **1992**, *71*, 235.
(33) Zhang, Q.; Bell, R.; Truong, T. N. *J. Phys. Chem.* **1995**, *99*, 592−599.
(34) Becke, A. D. *Phys. Rev. A* **1988**, *33*, 3098.
(35) Perdew, J. P. *Phys. Rev. B* **1986**, *33*, 8822.